Biosensors and Bioelectronics 26 (2011) 4337–4341

Contents lists available at ScienceDirect

Biosensors and Bioelectronics

journal homepage: www.elsevier.com/locate/bios

Nanoflake-like SnS_2 matrix for glucose biosensing based on direct electrochemistry of glucose oxidase

Zhanjun Yang, Yanyan Ren, Yongcai Zhang, Juan Li, Hongbo Li, Xiaochun Huang Xiaoya Hu*, Qin Xu

College of Chemistry and Chemical Engineering, Yangzhou University, Yangzhou 225002, PR China

ARTICLE INFO

Article history:
Received 27 January 2011
Received in revised form 11 April 2011
Accepted 20 April 2011
Available online 27 April 2011

Keywords:
Nanoflake-like SnS_2
Glucose oxidase
Direct electrochemistry
Glucose
Biosensor

ABSTRACT

A novel biosensor is developed based on immobilization of proteins on nanoflake-like SnS_2 modified glass carbon electrode (GCE). With glucose oxidase (GOD) as a model, direct electrochemistry of the GOD/nanoflake-like SnS_2 is studied. The prepared SnS_2 has large surface area and can offer favorable microenvironment for facilitating the electron transfer between protein and electrode surface. The properties of GOD/SnS_2 are characterized by scanning electron microscopy (SEM), X-ray diffraction (XRD), UV–vis spectroscopy, Fourier transform infrared spectroscopy (FTIR) and cyclic voltammetry (CV), respectively. The immobilized enzyme on nanoflake-like SnS_2 retains its native structure and bioactivity and exhibits a surface-controlled, reversible two-proton and two-electron transfer reaction with the apparent electron transfer rate constant (k_s) of 3.68 s^{-1}. The proposed biosensor shows fast amperometric response (8 s) to glucose with a wide linear range from 2.5×10^{-5} M to 1.1×10^{-3} M, a low detection limit of 1.0×10^{-5} M at signal-to-noise of 3 and good sensitivity (7.6 ± 0.5 mA M^{-1} cm^{-2}). The resulting biosensor has acceptable operational stability, good reproducibility and excellent selectivity and can be successfully applied in the reagentless glucose sensing at −0.45 V. It should be worthwhile noting that it opens a new avenue for fabricating excellent electrochemical biosensor.

1. Introduction

Recently, semiconductor nanomaterials have attracted increasing interests in the electrochemical sensing fields due to excellent properties (Vastarella and Nicastri, 2005; Sousa et al., 2010). In particular, metal oxide nanoparticles such as titanium oxide (Bao et al., 2008; Tang et al., 2010), iron oxide (Zhao et al., 2006), manganese oxide (Lvov et al., 2000), zinc oxide (Dai et al., 2009), zirconium oxide (Zhao et al., 2005) and nickel oxide (Salimi et al., 2007) have been used successfully for immobilizing enzymes or proteins to fabricate electrochemical biosensor. However, metal sulfide nanomaterials have been seldom reported to immobilize proteins for electrochemical biosensing.

SnS_2, an n-type semiconductors with a bandgap of 2.18–2.44 eV (Deshpande et al., 2007; Panda et al., 2007), consists of two layers of hexagonal closed packed sulfur anions with sandwiched tin cations, which are octahedrally coordinated by six nearest neighbor sulfur atoms. Each S is nested at the top of a triangle of Sn atom. Adjacent S–Sn–S layers are bound by weak van der Waals interactions (Wang et al., 2002). Due to good chemical stability, low cost and intriguing electrical and optical properties, SnS_2 has been become the promising material in light-sensitive photocatalyst (Yang et al., 2009), solar cells and opto-electronic devices (Deshpande et al., 2007; Panda et al., 2007), electrode for lithium-ion batteries (Kim et al., 2007; Seo et al., 2008) and gas sensor (Shi et al., 2006). As far as we know, SnS_2 has not been used as supporting material for fabricating electrochemical biosensors. Direct electron transfer (DET) in biological systems is a very important phenomenon for biochemical and biophysical sciences. However, the redox center in biomolecules is usually seated deeply in cavity of enzyme molecules (Meng et al., 2009). Great effort has been made to develop novel reagentless biosensor and biomedical devices based on DET of enzyme by immobilizing it on nanomaterials modified electrode (Deng et al., 2009; Nadzhafova et al., 2007; Shan et al., 2007). Many types of nanomaterials, such as gold nanoparticles (Jia et al., 2008; Liu and Ju, 2003; Pingarron et al., 2008), carbon nanotubes (Azamian et al., 2002; Liu et al., 2005, Deng et al., 2008), graphene (Kang et al., 2009; Shan et al., 2010a), titanium oxide (Bao et al., 2008; Tang et al., 2010), nickel oxide (Salimi et al., 2007) and zinc oxide (Dai et al., 2009) have been used to immobilize enzyme and promote DET of redox enzyme on the surface of electrode.

Glucose oxidase (GOD), an ideal mode enzyme for use in electrochemical biosensors, has been extensively employed for monitoring the blood glucose levels in diabetics on account of its catalytic ability to oxidize glucose (Shan et al., 2010b; Vamvakai et al., 2006; Xu et al., 2010). Here, nanoflake-like SnS_2 was pre-

* Corresponding author. Tel.: +86 514 87972034; fax: +86 514 87972034.
E-mail address: xyhu@yzu.edu.cn (X.H.X. Hu).

0956-5663/$ – see front matter © 2011 Elsevier B.V. All rights reserved.
doi:10.1016/j.bios.2011.04.031

pared and for the first time used to fabricate the enzyme biosensor based on DET of GOD. The small band gap of SnS_2 is favorable for conducting electrons from the biomolecules (Kang et al., 2009). A pair of well-defined redox peaks of GOD was obtained using GOD/SnS_2/nafion modified electrode. UV–vis and Fourier transform infrared (FTIR) spectrum demonstrate that nanoflake-like SnS_2 film can provide a favorable microenvironment for GOD to retain its native structure and bioactivity. The resulted biosensor with good reproducibility and excellent selectivity can be successfully applied in the reagentless glucose sensing and provides a promising alternative for electrochemical biosensing.

2. Materials and methods

2.1. Materials and reagents

GOD (EC 1.1.3.4, 108 U mg^{-1}, from *Aspergillus niger*) was purchased from Amresco. D-(+)-Glucose and Nafion were purchased from Sigma-Aldrich. Tin (II) chloride dehydrate ($SnCl_2{\cdot}2H_2O$) and sulfur (S) were supplied by Sinopharm Chemical Reagent Co., Ltd. A stock solution of D-glucose was prepared and allowed to mutarotate at room temperature for 24 h before measurements. Phosphate buffer solution (PBS) was 0.1 M Na_2HPO_4 and NaH_2PO_4 and its pH was adjusted with H_3PO_4 or NaOH solutions. All other chemicals and reagents are of analytical grade and were prepared using deionized distilled water.

2.2. Apparatus

Electrochemical measurements were performed on a CHI 852 C electrochemical workstation (Co., CHI, USA). All experiments were carried out with a three-electrode system with a glass carbon electrode (GCE, Ø = 3 mm) as the working electrode, a platinum wire as the auxiliary electrode and a saturated calomel electrode (SCE) as reference electrode. The cyclic voltammetric experiments were carried out at a scan rate of 50 mV s^{-1} in an electrochemical cell filled with 5.0 ml of PBS. All pH measurements were made with S-25 digital pH-meter with glass combination electrode.

Scanning electron micrographs (SEM) were obtained with a Hitachi S-4800 scanning electron microscope (Japan) at an acceleration voltage of 15 kV. X-ray diffraction (XRD) pattern was recorded on D8 Advance X-ray diffractometer (Bruker Co., Germany) at room temperature. FTIR spectra were measured with a Tensor 27 specrometer (Bruker Co., Germany). UV–vis spectra were recorded using UV-2550 spectrophotometer (Shimadzu Co., Japan).

2.3. Preparation of SnS_2 and enzyme electrodes

Nanoflake-like SnS_2 was simply synthesized according to previous method (Zhang et al., 2010). Briefly, the powders of $SnCl_2{\cdot}2H_2O$ and excess sublimed S were first mixed, ground for about 15 min and then transferred to a corundum crucible with a cover. The crucible with the reactants was heated in an electrothermal oven from room temperature to 200 °C at an average temperature increase rate of about 4.7 °C min^{-1}, kept at 200 °C for 10 h and then allowed to cool to room temperature. The resulting powder was washed with carbon disulfide; deionizer distilled water and ethanol, respectively, and dried in air at 80 °C and finally yellow nanoflake-like SnS_2 was obtained.

The GCE was firstly polished successively with 0.3 and 0.5 μm alumina slurry (Buhler) followed by rinsing thoroughly with deionizer distilled water, successive sanitation in 1:1 nitric acid, acetone and deionizer distilled water and dried in air. 1.0 mg SnS_2 was dispersed in 1.0 ml deionized distilled water with ultra-sanitation. 5.0 μl of the suspension was dropped on the surface of the pretreated GCE and dried in silica gel desiccators. 5.0 μl of 5 mg ml^{-1} GOD solution was then dropped on the SnS_2 modified GCE and dried silica gel desiccators. After 5.0 μl of 1% Nafion solution was dropped on the GOD/SnS_2 modified electrode surface, the GOD/SnS_2/Nafion modified electrode was obtained. The modified electrode was rinsed throughout with doubly distilled water to wash away the loosely adsorbed enzyme molecules. When not in use, the fabricated electrode was stored in 0.1 M pH 7.0 PBS at 4 °C in a refrigerator.

3. Results and discussion

3.1. Characterizations of SnS2, GOD and GOD/SnS2

In this work, nanoflake-like SnS_2 was synthesized and further used to modify GEC for the immobilization of GOD. Fig. 1A shows the SEM image of the synthesized SnS_2, which displays an anisotropic and uniform flake-like morphology with about 40 nm flake thickness. As seen from the XRD patterns of Fig. 1B, the as-synthesized product displays only the XRD peaks corresponding to hexagonal-phase SnS_2 (JCPDS card no. 89-2358), indicating that phase-pure SnS_2 powders have been successfully obtained (Zhang et al., 2010).

UV–vis spectroscopy is a useful tool to study the possible conformational change of GOD in nanoflake-like SnS_2 film. Fig. 2A shows the UV–vis absorption spectra of SnS_2 (curve a), GOD (curve b) and GOD/SnS_2 (curve c). In the case of GOD, the absorption band at 278 nm and two weak peaks at 380 and 458 nm are attributed to the characteristic of polypeptide chains and the oxidized form of flavin group in protein structure, respectively (Liu and Hu, 2007). The position and shape of absorption bands for GOD/SnS_2 are almost the same as those of pure GOD, suggesting that the GOD immobilized in nanoflake-like SnS_2 indeed maintains its native structure (Shan et al., 2010a).

FTIR spectroscopy was used to characterize the existing state of the immobilized enzyme. Fig. 2B shows the FTIR spectra of the SnS_2 (curve a), native GOD (curve b) and GOD immobilized on SnS_2 film (curve c). For the pure SnS_2, no obvious absorption peak was observed. The FTIR spectrum of native GOD shows two characteristic peaks at 1615 and 1547 cm^{-1}, which are attributed to amide I and II bands of protein. Compare to curve b, the FTIR spectrum of GOD/SnS_2 also shows two absorption peaks at 1643 and 1569 cm^{-1} corresponding to amide I and II bands, indicating that GOD has been successfully immobilized on the SnS_2 film (Shi et al., 2003). The position of absorption bands corresponding to amide I and II bands for native GOD and GOD immobilized on SnS_2 has some differences, indicating that there may be intermolecular interaction between enzyme and nanoflake-like SnS_2 (Fan et al., 2007).

3.2. Direct electrochemistry of GOD/SnS_2/Nafion-modified GCE

Due to the redox reaction of FAD in the GOD molecule, the electrochemistry response of GOD immobilized on the solid surface is known to undergo two protons and two electrons process (Ianniello et al., 1982; Liu and Ju, 2003). Under proper conditions, DET between GOD and substrate can be observed from the electrochemical response and used to fabricate electrochemical biosensor (Deng et al., 2009; Kang et al., 2009; Nadzhafova et al., 2007; Shan et al., 2010b). Fig. 3 shows the cyclic voltammograms of different films modified GCE in 0.1 M N_2-saturated PBS at a scan rate of 50 mV s^{-1}. No peaks were observed for Nafion/GCE (Fig. 3a) and SnS_2/Nafion/GCE (Fig. 3b). The background current of SnS_2/GCE is higher than that of bare GCE, which is attributed to the large surface area of nanoflake-like SnS_2 (Kang et al., 2009). Compared to the GOD modified GCE, GOD immobilized on nanoflake-like SnS_2 shows a pair of distinct and well-defined redox peaks at

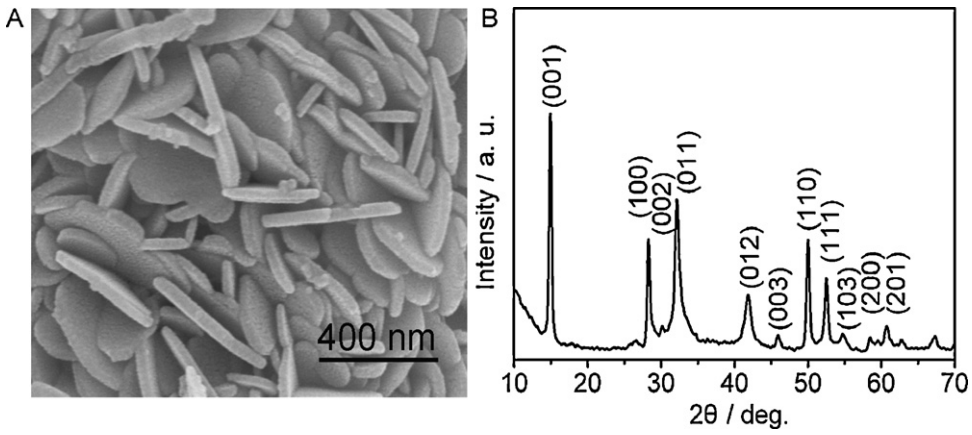

Fig. 1. SEM image (A) and XRD pattern (B) of the nanoflake-like SnS_2.

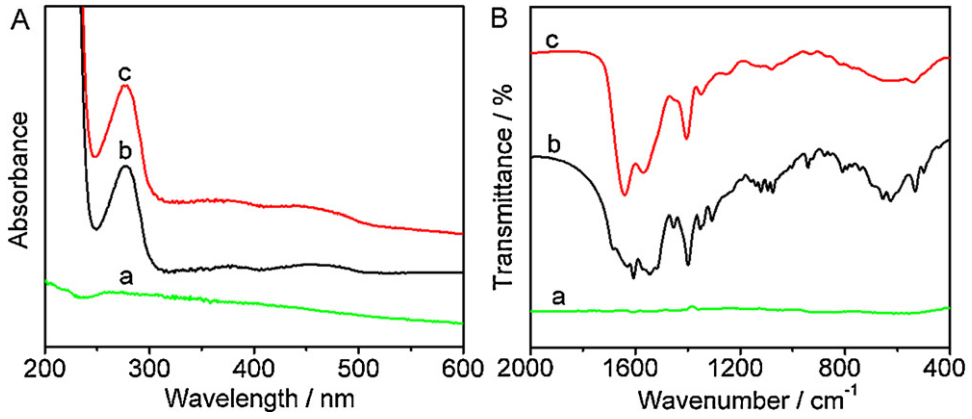

Fig. 2. UV–vis absorption spectra (A) and FTIR spectra of (B) of SnS_2 (a), GOD (b) and GOD/SnS_2.

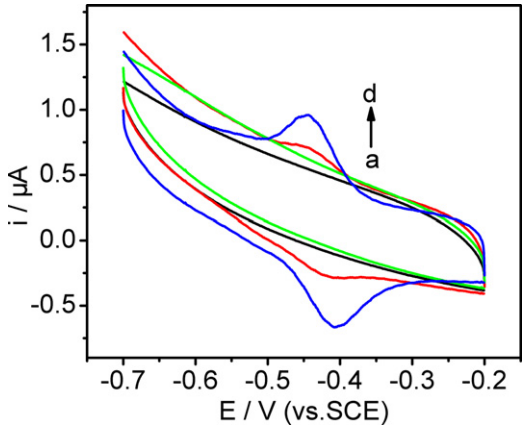

Fig. 3. Cyclic voltammograms for (a–d) bare/GCE, SnS_2/Nafion/GCE, GOD/Nafion/GCE and GOD/SnS_2/Nafion/GCE in N_2-saturated 0.1 M pH 7.0 PBS at a scan rate of 50 mV s^{-1}.

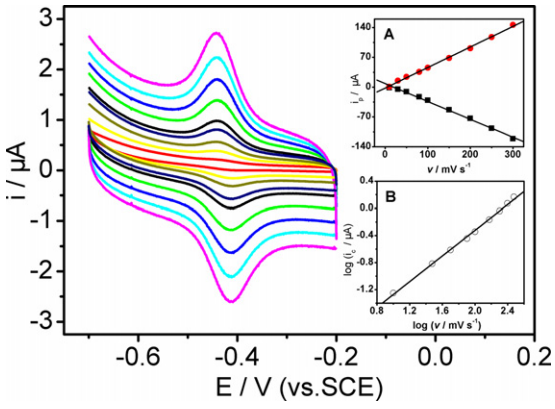

Fig. 4. Cyclic voltammograms of the GOD/SnS_2/Nafion/GCE in N_2-saturated 0.1 M pH 7.0 PBS at 10, 30, 50, 80, 100, 150, 200, 250 and 300 mV s^{-1} (from inner to outer). Inset A: plots of anodic and cathodic peak currents vs. scan rates. Inset B: plot of logarithm of i_{pc} vs. logarithm of ν^{-1}.

−0.409 V and −0.442 V. Obviously, the modified nanoflake-like SnS_2 ensures effective electrical contact between redox-active centers of enzyme and electrode surface, which leads to the direct electrochemistry of GOD (Willner et al., 2006). The peak potential separation is 33 mV, which is much smaller than that of 80 mV at GOD/graphene–chitosan/GCE (Kang et al., 2009), suggesting the faster DET between the redox-active site of GOD (the cofactor FAD) and GCE without the help of electron transfer mediator (Deng et al., 2009).

The effect of the scan rate on the cyclic voltammetric performance at the GOD/SnS_2/Nafion/GCE was shown in Fig. 4. With the increase of the scan rate, the redox potentials of GOD shift slightly. The anodic and cathodic peak currents linearly increased with the increasing scan rate from 10 to 300 mV s^{-1} (inset A of Fig. 4), indicating that the redox reaction of GOD on nanoflake-like SnS_2 modified electrode is a quasi-reversible surface-controlled process. The logarithm plot of cathodic peak current versus logarithm of the san rate shows a linear relationship (inset B of Fig. 4) with a correlation coefficient of 0.9989 and a slope of 0.9505, which

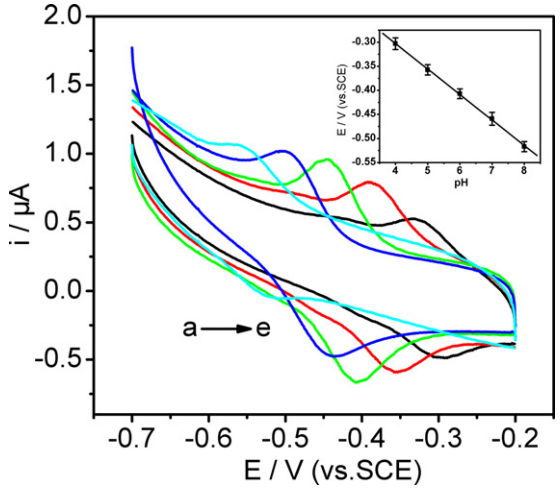

Fig. 5. Cyclic voltammograms of the GOD/SnS_2/Nafion/GCE in N_2-saturated PBS with different pH values of (a–e) 4.0, 5.0, 6.0, 7.0 and 8.0 at a scan rate of 50 mV s^{-1}. Inset: Plot of formal potentials vs. pH.

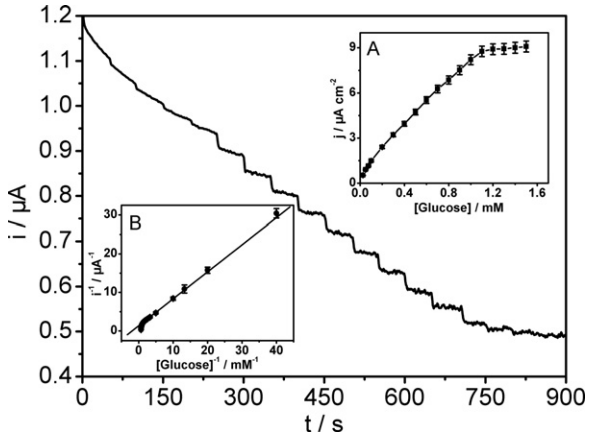

Fig. 6. Typical steady-state response of the GOD/SnS_2/Nafion/GCE on successive addition of glucose into air-saturated 0.1 M pH 6.0 PBS, applied potential, −0.45 V. Inset A: Calibration curve of the GOD/SnS_2/Nafion/GCE for glucose. Inset B: plot of i^{-1} vs. [glucose]$^{-1}$.

is very close to the theoretical slope for thin layer electrochemical behavior (Shan et al., 2010a). According to Laviron's equation (Laviron, 1979), the charge-transfer coefficient and the apparent electron transfer rate constant (k_s) for the proposed electrode were calculated to be 0.5 and 3.68 s^{-1}, respectively. The obtained value of k_s is larger than those of 1.56 s^{-1} at boron-doped carbon nanotubes (Deng et al., 2008), 1.7 s^{-1} at multi-walled carbon nanotubes (Guiseppi-Elie et al., 2002), 2.83 s^{-1} at graphene–chitosan modified GCE (Kang et al., 2009). This result further confirms that nanoflake-like SnS_2 facilitates the fast electron transfer between redox-active site of enzyme and the surface of electrode.

The surface coverage (Γ^*) of the electroactive GOD on surface of the modified electrode can be calculated from the charge integration of cathodic peak in CVs at 50 mV s^{-1}, according to $\Gamma^* = Q/nFA$, where Q is the charge consumed in the reaction, n is the number of electrons transferred, F is the Farady constant, and A is the electrode area. The surface coverage was calculated to be 1.60×10^{-11} mol cm^{-2}, which is larger than those of 9.8×10^{-12} mol cm^{-2} at GOD/Au nanoparticles/carbon paste electrode (Liu and Ju, 2003), 7.82×10^{-12} mol cm^{-2} at GOD/Au-dihexadecyl phosphate modified electrode (Wu and Hu, 2007) and 2.86×10^{-12} mol cm^{-2} at bare GCE (Zhang et al., 2007), indicating saturated absorption of multilayers GOD in nanoflake-like SnS_2 film.

The influence of the pH value on the electrochemical behavior of GOD on nanoflake-like SnS_2 was investigated. As shown from Fig. 5, an increase of solution pH from 4.0 to 8.0 resulted in a negative shift of both the cathodic and anodic peak potentials. The redox potentials of GOD/SnS_2/Nafion modified GCE changed linearly as a function of solution pH with a slope of −58.3 mV pH^{-1} for the reduction process. This slope is close to the theoretical value of −58.6 mV pH^{-1} (Deng et al., 2009), indicating two protons and two electrons participating in the electron transfer process.

3.3. Performance of the proposed glucose biosensor

In air-saturated PBS, no peak was observed at SnS_2/Nafion modified GCE (curve b, Fig. S1A in Supporting information), though an increase in cathodic current at the potentials more negative than −0.4 V. Curves d and e in Fig. S1B (Supporting Information) showed the cyclic voltammograms of GOD/SnS_2/Nafion modified GCE in oxygen-free and air-saturated PBS, respectively. A great increase in reduction peak current and a simultaneous decrease in oxidation current of GOD in the presence of oxygen can be observed, demonstrating an obvious electrocatalytic process toward the reduction of dissolved oxygen according to the following equations (Liu and Ju, 2003):

$$\mathrm{GOD(FAD)} + 2e^- + 2H^+ \leftrightarrow \mathrm{GOD(FADH_2)} \quad (1)$$

$$\mathrm{GOD(FADH_2)} + O_2 \rightarrow \mathrm{GOD(FAD)} + H_2O_2 \quad (2)$$

In the presence of oxygen, regenerated GOD (FAD) resulted in the increase of the reduction peak current of FAD. When glucose was added into this system, it restrained the electrocatalytic reaction due to the enzyme-catalyzed reaction, which reduced the concentration of GOD (FAD) as shown in the following equation:

$$\mathrm{Glucose} + \mathrm{GOD\,(FAD)} + O_2 \rightarrow \mathrm{Gluconolactone} + \mathrm{GOD\,(FADH_2)} \quad (3)$$

Thus the reduction peak current decreased with the increase of glucose concentration, (curve f and g, Fig. S1B in Supporting information), while no obvious change was observed at SnS_2/Nafion modified GCE (curve c, Fig. S1A in Supporting information). Based on the decease, the glucose biosensor was proposed.

The potential of −0.45 V and pH value of 6.0 were chosen as the optimal conditions for the amperomeric determination of glucose. Fig. 6 showed the typical amperometric response curves at GOD/SnS_2/Nafion modified GCE on successive injection of glucose to the air-saturated stirring PBS. The proposed electrode achieved 95% of the steady-state current within 8 s. The response increased linearly with the increase of glucose concentration ranging from 2.5×10^{-5} M to 1.1×10^{-3} M with a low detection limit of 1.0×10^{-5} M at signal-to-noise of 3 (inset A of Fig. 6). The sensitivity for GOD/SnS_2/GCE was calculated to be 7.6 ± 0.05 mA M^{-1} cm^{-2}), which was higher than 0.2, 1.06, 4.8, 0.053 mA M^{-1} cm^{-2} for the glucose biosensor based on multi-walled carbon nanotubes (Salimi et al., 2004), singe-walled carbon nanohorns (Liu et al., 2008), laponite nanoparticles (Shan et al., 2010b) and highly ordered mesoporous carbon foams (Zhou et al., 2008). The reproducibility of the proposed biosensor was investigated using 0.1 mM glucose by successive detection for 30 times. The relative standard deviation (RSD) was 5.7%, indicating a good reproducibility. After 40 successive detecting the response was still retained 96% value of the initial response, suggesting the acceptable operational stability of the proposed biosensor. After a storage period of 20 days in 0.1 M pH 7.0 PBS at 4 °C, the fabricated biosensor showed an 8% loss of bioactivity. These results indicate that the immobilized GOD retains its high enzymatic activity and the nanoflake-like SnS_2 film provides a favorable microenvironment for GOD to perform DET at the modified electrode.

Based on the slope and the intercept of the plot of the reciprocals of the steady-state current versus glucose concentration (inset B of Fig. 6), the apparent Michaelis–Menten constant (K_M^{app}) was calculated to be 1.16 mM for the GOD/SnS_2/Nafion/GCE. The (K_M^{app}) values is much smaller than those of 4.4, 11.6 mM and 37.6 mM for immobilized GOD (Kang et al., 2009; Uang and Chou, 2003; Zheng et al., 2002), indicating that the GOD immobilized on SnS_2 had high affinity to glucose.

3.4. Interference study

The interferences on glucose detection were evaluated using 0.1 mM uric acid (UA) and 0.1 mM ascorbic acid (AA) at the applied potential of −0.45 V (Fig. S2B in Supporting information). Upon addition of 0.1 mM glucose in PBS, an obvious current response appeared. When successively injecting the AA and UA into the solution, no obvious increase of the current was observed. After the addition of 0.1 mM glucose again, the current value was close to that determined in absence of interferents. These results demonstrates that the proposed biosensor has high selectivity for glucose in the presence of those endogenously coexisted electroactive substances.

3.5. Detection of glucose in practical serum sample

The detection of glucose in serum was performed without any sample pretreatment except a dilution step. The glucose level was determined to be 4.26 close to 4.45 mM obtained by spectrophotometry. The recoveries for assay of 0.1–0.5 mM glucose added in serum samples were between 97% and 105% for five measurements, demonstrating good accuracy for detection of glucose in real samples.

4. Conclusions

In this work, nanoflake-like SnS_2 has been prepared for the immobilization of protein and glucose biosensing. Nanoflake-like SnS_2 with larger specific surface area shows a favorable microenvironment for facilitating the electron transfer between protein and electrode surface. The immobilized enzyme on nanoflake-like SnS_2 retains its native structure and bioactivity and exhibits fast amperometric response to glucose. The constructed enzyme biosensor has excellent selectivity, good sensitivity and reproducibility, and can be successfully applied in the reagentless glucose sensing. The nanoflake-like SnS_2 provides a new approach and efficient matrix for promoting the direct electron transfer of proteins and developing novel types of biosensors.

Acknowledgments

This work was financially supported by from National Natural Science Foundation of China (20875081, 21075107, 21005070, 20705030), projects of the 863 Plan (2009AA03Z331) and the University Natural Science Foundation of Jiangsu Province (08KJB150019).

Appendix A. Supplementary data

Supplementary data associated with this article can be found, in the online version, at doi:10.1016/j.bios.2011.04.031.

References

Azamian, B.R., Davis, J.J., Coleman, K.S., Bagshaw, C.B., Green, M.L.H., 2002. J. Am. Chem. Soc. 124, 12664–12665.
Bao, S.J., Li, C., Zang, J.F., Cui, X.Q., Qiao, Y., Guo, J., 2008. Adv. Funct. Mater. 18, 591–599.
Dai, Z.H., Shao, G.J., Hong, J.M., Bao, J.C., Shen, J., 2009. Biosens. Bioelectron. 24, 1286–1291.
Deshpande, N.G., Sagade, A.A., Gudage, Y.G., Lokhande, C.D., 2007. J. Alloys Compd. 436, 421–426.
Deng, C.Y., Chen, J.H., Chen, X.L., Xiao, C.H., Nie, L.H., Yao, S.Z., 2008. Biosens. Bioelectron. 23, 1272–1277.
Deng, S.Y., Jian, G.Q., Lei, J.P., Hu, Z., Ju, H.X., 2009. Biosens. Bioelectron. 25, 373–377.
Fan, Q., Shan, D., Xue, H.G., He, Y.Y., Cosnier, S., 2007. Biosens. Bioelectron. 22, 816–821.
Guiseppi-Elie, A., Lei, C., Baughman, R.H., 2002. Nanotechnology 13, 559–564.
Ianniello, R.M., Lindsay, T.J., Yacynych, A.M., 1982. Anal. Chem. 54, 1098–1101.
Jia, F., Shan, C.S., Li, F.H., Niu, L., 2008. Biosens. Bioelectron. 24, 945–950.
Kang, X.H., Wang, J., Wu, H., Aksay, I.A., Liu, J., Lin, Y.H., 2009. Biosens. Bioelectron. 25, 901–905.
Kim, T.J., Kim, C., Son, D., Choi, M., Park, B., 2007. J. Power Sources 167, 529–535.
Laviron, E., 1979. J. Electroanal. Chem. 101, 19–28.
Liu, H.Y., Hu, N.F., 2007. Electroanalysis 19, 884–892.
Liu, S.Q., Ju, H.X., 2003. Biosens. Bioelectron. 19, 177–183.
Liu, X., Shi, L., Niu, W., Li, H., Xu, G., 2008. Biosens. Bioelectron. 23, 1887–1890.
Liu, Y., Wang, M.K., Zhao, F., Hu, Z.A., Dong, S.J., 2005. Biosens. Bioelectron. 21, 984–988.
Lvov, Y., Munge, B., Giraldo, O., Ichinose, I., Suib, S.L., Rusling, J.F., 2000. Langmuir 16, 8850–8857.
Meng, L., Jin, J., Yang, G.X., Lu, T.H., Zhang, H., Cai, C.X., 2009. Anal. Chem. 81, 7271–7280.
Nadzhafova, O., Etienne, M., Walcarius, A., 2007. Electrochem. Commun. 9, 1189–1195.
Panda, S.K., Antonakos, A., Liarokapis, E., Bhattacharya, S., Chaudhuri, S., 2007. Mater. Res. Bull. 42, 576–583.
Pingarron, J.M., Yanez-Sedeno, P., Gonzalez-Cortes, A., 2008. Electrochim. Acta 53, 5848–5866.
Seo, J., Jang, J., Park, S., Kim, C., Park, B., Cheon, J., 2008. Adv. Mater. 20, 4269–4273.
Shan, C.S., Yang, H.F., Han, D.X., Zhang, Q., Ivaska, A., Niu, L., 2010a. Biosens. Bioelectron. 25, 1070–1074.
Shan, D., Zhu, M.J., Han, E., Xue, H.G., Cosnier, S., 2007. Biosens. Bioelectron. 23, 648–654.
Shan, D., Zhang, J., Xue, H.G., Ding, S.N., Cosnier, S., 2010b. Biosens. Bioelectron. 25, 1427–1433.
Shi, C., Liu, Q., Xie, Y., Xu, X., 2003. J. Mol. Struct. 644, 139–144.
Shi, W., Huo, L., Wang, H., Zhang, H., Yang, J., Wei, P., 2006. Nanotechnology 17, 2918–2924.
Salimi, A., Compton, R.G., Hallaj, R., 2004. Anal. Biochem. 333, 49–56.
Salimi, A., Sharifi, E., Noorbakhsh, A., Soltanian, S., 2007. Biosens. Bioelectron. 22, 3146–3153.
Sousa, C.P., Polo, A.S., Torresi, R.M., de Torresi, S.I.C., Alves, W.A., 2010. J. Colloid Interface Sci. 346, 442–447.
Tang, H., Yan, F., Tai, Q.D., Chan, H.L.W., 2010. Biosens. Bioelectron. 25, 1646–1651.
Uang, Y., Chou, T.C., 2003. Biosens. Bioelectron. 20, 2435–2453.
Vamvakai, V., Tsagaraki, K., Chaniotakis, N., 2006. Anal. Chem. 78, 5538–5542.
Vastarella, W., Nicastri, R., 2005. Talanta 66, 627–633.
Wang, C., Tang, K., Yang, Q., Qian, Y., 2002. Chem. Phys. Lett. 357, 371–375.
Willner, B., Katz, E., Willner, I., 2006. Curr. Opin. Biotechnol. 17, 589–596.
Wu, Y.H., Hu, S.S., 2007. Bioelectrochemistry 70, 335–341.
Xu, X.A., Jiang, S.J., Hu, Z., Liu, S.Q., 2010. ACS Nano 4, 4292–4298.
Yang, C., Wang, W., Shan, Z., Huang, F., 2009. J. Solid State Chem. 182, 807–812.
Zhang, J.D., Feng, M.L., Tachikawa, H., 2007. Biosens. Bioelectron. 22, 3036–3041.
Zhang, Y.C., Du, Z.N., Li, S.Y., Zhang, M., 2010. Appl. Catal. B: Environ. 95, 153–159.
Zhao, G., Feng, J.J., Xu, J.J., Chen, H.Y., 2005. Electrochem. Commun. 7, 724–729.
Zhao, G., Xu, J.J., Chen, H.Y., 2006. Electrochem. Commun. 8, 148–154.
Zheng, H., Xue, H., Zhang, Y., Shen, Z., 2002. Biosens. Bioelectron. 17, 541–545.
Zhou, M., Shang, L., Li, B., Huang, L., Dong, S., 2008. Biosens. Bioelectron. 24, 442–447.